Profile of Changes in Lipid Bilayer Structure Caused by β-Amyloid Peptide[†]

John J. Kremer, Daniel J. Sklansky, and Regina M. Murphy*

Department of Chemical Engineering, University of Wisconsin−Madison, Madison, Wisconsin 53706-1607

Received February 28, 2001; Revised Manuscript Received May 22, 2001

ABSTRACT: β-Amyloid peptide (Aβ) is the primary constituent of senile plaques, a defining feature of Alzheimer's disease. Aggregated Aβ is toxic to neurons, but the mechanism of toxicity is uncertain. One hypothesis is that interactions between Aβ aggregates and cell membranes mediate Aβ toxicity. Previously, we described a positive correlation between the Aβ aggregation state and surface hydrophobicity, and the ability of the peptide to decrease fluidity in the center of the membrane bilayer [Kremer, J. J., et al. (2000) *Biochemistry 39,* 10309−10318]. In this work, we report that Aβ aggregates increased the steady-state anisotropy of 1,6-diphenyl-1,3,5-hexatriene (DPH) embedded in the hydrophobic center of the membrane in phospholipids with anionic, cationic, and zwitterionic headgroups, suggesting that specific charge−charge interactions are not required for Aβ−membrane interactions. Aβ did not affect the fluorescence lifetime of DPH, indicating that the increase in anisotropy is due to increased ordering of the phospholipid acyl chains rather than changes in water penetration into the bilayer interior. Aβ aggregates affected membrane fluidity above, but not below, the lipid phase-transition temperature and did not alter the temperature or enthalpy of the phospholipid phase transition. Aβ induced little to no change in membrane structure or water penetration near the bilayer surface. Overall, these results suggest that exposed hydrophobic patches on the Aβ aggregates interact with the hydrophobic core of the lipid bilayer, leading to a reduction in membrane fluidity. Decreases in membrane fluidity could hamper functioning of cell surface receptors and ion channel proteins; such decreases have been associated with cellular toxicity.

Alzheimer's disease (AD)[1] is the most widespread progressive neurodegenerative disease, characterized in part by the presence of cerebrovascular amyloid deposits and senile plaques. The principal proteinaceous component of these plaques is β-amyloid (Aβ), a 39−43-amino acid peptide. Aβ is a cleavage product of the large, membrane-anchored amyloid precursor protein (APP). The Aβ peptide consists of 28 amino acids from the extracellular portion of APP and 11−15 amino acids that reside in the transmembrane domain. This amphiphilic peptide spontaneously forms aggregates in aqueous solutions at or below physiological pH.

In vitro, Aβ toxicity is closely correlated with aggregation into cross-β-sheet fibrils (*1*, *2*). The mechanism behind Aβ toxicity has been debated; for review, see Mattson (*3*) or Iversen et al. (*4*). The hypothesis that interactions between Aβ aggregates and neuronal membranes play an important role in toxicity is gaining some acceptance (*5*). Recently, Aβ(1−42) aggregates in a membrane-bound conformation have been discovered in dog and human brain sections (*6*, *7*). Several possible mechanisms by which Aβ−membrane interactions are toxic have been suggested, including perturbations in membrane fluidity (*8*−*11*), free radical production and lipid peroxidation (*12*), formation of ion channels (*13*, *14*), changes in lipid metabolism (*15*), and increased phospholipase activity (*16*, *17*).

Although the connection between Aβ−membrane interactions and toxicity remains tenuous, the existence of these interactions has been well established. Specifically, Aβ aggregation kinetics and pathways can be altered in the presence of various membrane components (*18*−*20*). Aβ has been variously reported to alter intramembraneous structure in cultured PC-12 cells (*21*), increase permeability in lysosomal and endosomal vesicles (*22*), induce small unilamellar liposome fusion (*23*), insert into negatively charged lipid bilayers (*24*), interact with ganglioside-containing membranes (*18*, *25*), and induce leakage of encapsulated dyes (*26*). A few researchers have explored whether Aβ must be aggregated to interact with membranes. Only aggregated Aβ bound to rat cortical homogenates in vitro (*27*), and Aβ-(25−35) induced membrane leakage and currents only if sufficiently aggregated (*28*).

Previously, we determined the effect of Aβ aggregate size and hydrophobicity on the fluidity of phospholipid vesicles in contact with Aβ aggregates by measuring the fluorescence

[†] Funding included grants from the National Institute of Aging (AG14079), an SC Johnson Distinguished Fellowship, and NIH Chemistry-Biology Interface Training Grant 5 T32 GM08505 (J.J.K.).

* To whom correspondence should be addressed. Phone: (608) 262-1587. Fax: (608) 262-5434. E-mail: murphy@engr.wisc.edu.

[1] Abbreviations: Aβ, β-amyloid peptide (1−40); AD, Alzheimer's disease; APP, amyloid precursor protein; BSA, bovine serum albumin; CA, carbonic anhydrase; chol, cholesterol; DMPC, 1,2-dimyristoyl-*sn*-glycero-3-phosphocholine; DMPG, 1,2-dimyristoyl-*sn*-glycero-3-[phospho-*rac*-(1-glycerol)]; DMSO, dimethyl sulfoxide; DOTAP, 1,2-dioleoyl-3-(trimethylammonium)propane; DPH, 1,6-diphenyl-1,3,5-hexatriene; DSC, differential scanning calorimetry; GP, generalized polarization; ΔH, gel to liquid-crystalline phase-transition enthalpy; HPLC, high-pressure liquid chromatography; laurdan, 6-dodecanoyl-2-(dimethylamino)naphthalene; *L*:*P*, lipid:peptide ratio; PBSA, phosphate-buffered saline with azide, 10 mM KH_2PO_4/K_2HPO_4, 150 mM NaCl, and 0.02% NaN_3; POPC, 1-palmitoyl-2-oleoyl-*sn*-glycero-3-phosphocholine; POPE, 1-palmitoyl-2-oleoyl-*sn*-glycero-3-phosphoethanolamine; POPG, 1-palmitoyl-2-oleoyl-*sn*-glycero-3-[phospho-*rac*-(1-glycerol)]; POPS, 1-palmitoyl-2-oleoyl-*sn*-glycero-3-phospho-L-serine; $\langle\tau\rangle$, mean DPH fluorescence lifetime; T_m, gel to liquid-crystalline phase-transition temperature; TMA-DPH, 1-[4-(trimethylammonium)phenyl]-6-phenyl-1,3,5-hexatriene *p*-toluenesulfonate.

10.1021/bi010417x CCC: $20.00
Published on Web 06/28/2001

anisotropy of the membrane-embedded dye DPH (*8*). Aβ aggregation state and surface hydrophobicity were positively correlated with the ability of the Aβ aggregates to decrease fluidity in the center of the membrane bilayer. In work reported here, these initial studies are expanded to include several additional phospholipids as well as variation in the depth of the fluorescent probe in the bilayer. We employ the fluorescent dyes DPH, 1-[4-(trimethylammonium)phenyl]-6-phenyl-1,3,5-hexatriene *p*-toluenesulfonate (TMA-DPH), and 6-dodecanoyl-2-(dimethylamino)naphthalene (laurdan) to probe distinct regions of the bilayer (*29*−*32*). TMA-DPH is a trimethylamino-modified derivative of DPH, while laurdan is an amphiphilic fluorescent probe that resides at the hydrophilic−hydrophobic interface of the lipid bilayer (*33*). The additional lipids that are employed are 1,2-dioleoyl-3-(trimethylammonium)propane (DOTAP), 1,2-dimyristoyl-*sn*-glycero-3-phosphocholine (DMPC), and 1,2-dimyristoyl-*sn*-glycero-3-[phospho-*rac*-(1-glycerol)] (DMPG). We selected DOTAP for its cationic headgroup, yet its gel to liquid-crystalline phase-transition temperature (T_m) is similar to those of POPC and POPG (−10 vs −2 °C). DMPC and DMPG were chosen because they undergo a phase transition near room temperature.

Our goals included (i) investigating interactions between positively charged lipids and Aβ aggregates, (ii) using lifetime fluorescence spectroscopy to confirm the finding that Aβ aggregates decrease membrane fluidity, (iii) exploring the relationship between phospholipid bilayer phase transitions and Aβ−membrane interactions, and (iv) probing Aβ−membrane interactions near the bilayer surface as well as in the hydrophobic core. We report that aggregated Aβ increased DPH anisotropy in cationic DOTAP lipids in a fashion similar to the effect on anionic and zwitterionic lipids. Aggregated Aβ did not change the average DPH fluorescence lifetime; therefore, the increased DPH anisotropy is indicative of an increased ordering of the phospholipid bilayer. Aβ decreased the fluidity of phospholipid bilayers only in their liquid-crystalline state and did not affect the T_m or gel to liquid-crystalline phase-transition enthalpy (ΔH). Aβ aggregates decreased membrane fluidity significantly more in the hydrophobic core of the bilayer than near the hydrophobic−hydrophilic interface.

EXPERIMENTAL PROCEDURES

Materials. Synthetic Aβ(1−40) peptide was purchased from AnaSpec Inc. (San Jose, CA). Cleavage of APP yields Aβ peptides of 39−43 residues, with Aβ(1−40) representing the largest percentage in biological samples (*34*). Several Aβ batches were used with no noticeable change in properties. Purities were >95% as verified by HPLC, and mass spectrometry confirmed correct molecular masses. Lyophilized Aβ was stored at −70 °C until it was used.

1-Palmitoyl-2-oleoyl-*sn*-glycero-3-phosphocholine (POPC), 1-palmitoyl-2-oleoyl-*sn*-glycero-3-phosphoethanolamine (POPE), 1-palmitoyl-2-oleoyl-*sn*-glycero-3-[phospho-*rac*-(1-glycerol)] (POPG), 1-palmitoyl-2-oleoyl-*sn*-glycero-3-phospho-L-serine (POPS), DMPC, DMPG, DOTAP, and cholesterol (chol) were purchased from Avanti Polar Lipids (Alabaster, AL). Laurdan and TMA-DPH were purchased from Molecular Probes (Eugene, OR). HPLC (99.9%) grade dimethyl sulfoxide (DMSO), poly-L-lysine (molecular mass of 280 000 Da), bovine serum albumin (BSA), mixed gangliosides, bovine type 2 carbonic anhydrase (CA), and DPH were purchased from Sigma Chemical Co. (St. Louis, MO). Lipids were stored at −20 °C in chloroform. Cholesterol and gangliosides were stored as lyophilized solids at −20 °C.

Aβ Sample Preparation. Aβ was prepared essentially as described previously (*8*). Briefly, Aβ was dissolved for no less than 60 min at 10 mg/mL in filtered (0.2 μm) DMSO, which was previously dried using molecular sieves (Sigma). This treatment disrupts β-sheet structure (*35*) and renders Aβ apparently monomeric (unpublished data and ref *36*). An Aβ stock solution was diluted 20-fold in PBSA (pH 6 or 7) and allowed to aggregate for 2 days at room temperature at 0.5 mg/mL (~115 μM equivalent monomer concentration). Freshly diluted Aβ samples were kept in DMSO (at 10 mg/mL) until direct dilution into the sample was carried out.

Liposome Preparation. Single-component and multicomponent large unilamellar vesicles were prepared by extrusion. Multicomponent type 1 and type 2 vesicles consist of POPC, POPE, POPS, and chol (36:36:10:18 by mass) and POPC, POPE, POPS, chol, and gangliosides (33:33:10:16:8 by mass). Chol and gangliosides were dissolved in chloroform and/or methanol and mixed with phospholipids stored in chloroform. DPH, TMA-DPH, and laurdan were dissolved in chloroform and/or methanol and added to the lipid solutions at a 1:500 (dye:lipid) molar ratio, except for DPH lifetime measurements where DPH was added at a 1:200 ratio. The lipid/dye solutions were dried using a N_2 stream, followed by vacuum desiccation for 1 h and overnight storage in a desiccated container. Dried samples were stored at −20 °C. Lipid solutions were resuspended in PBSA, allowed to equilibrate for at least 30 min, and passed through an extruder (Avanti Polar Lipids) with a 100 nm pore size membrane at least 19 times. This generates liposomes ~100−125 nm in diameter, as confirmed by dynamic light scattering measurements. POPC, POPG, DOTAP, and type 1 and 2 lipids were extruded at room temperature. DMPC and DMPG lipids were dissolved and extruded at high temperatures (~35−45 °C). Exposure to light was minimized during the drying and extrusion processes. Liposome solutions were either used immediately or stored in the dark at 4 °C for up to 3 days.

Fluorescence Measurements. DPH and TMA-DPH anisotropy measurements were taken using a PTI (South Brunswick, NJ) spectrofluorometer equipped with manual polarizers, a four-cuvette turret, and a circulating thermostated water bath (Fisher Scientific, Pittsburgh, PA). Cuvette temperatures were taken using a digital thermometer (Fisher Scientific). Excitation and emission wavelengths were 360 and 430 nm, respectively. Data were averaged over 4 s for each cuvette. Alignment was verified using a dilute glycogen solution ($P > 0.95$). *G* factors were calculated as described elsewhere (*37*). *G* factors varied slightly with temperature, so separate *g* factors were calculated at each cuvette temperature. Anisotropy (*r*) was calculated with eq 1:

$$r = \frac{I_{par} - gI_{per}}{I_{par} - 2gI_{per}} \quad (1)$$

where I_{par} and I_{per} are parallel and perpendicular fluorescence intensities, respectively, and *g* is the *g* factor. The maximum

observable DPH anisotropy in membranes is limited to 0.30−0.34 (*38*).

Anisotropy was determined as a function of either Aβ concentration (for Aβ titration experiments) or cuvette temperature. For Aβ titration experiments, the lipid/dye solutions were diluted to 250 μM lipid using PBSA (pH 6 or 7). The pH of the lipid solution was always matched with the pH of the Aβ solution. Aliquots of Aβ solutions were then titrated directly into the fluorescence cuvette, and measurements were taken after steady-state conditions were reached (∼10−20 min). For temperature experiments, the phospholipid solution was diluted to 250 μM in the presence of either Aβ (final Aβ concentration of 18.5 μM) or additional PBSA. Solutions were equilibrated to the set-point temperature before each measurement. Controls for both types of experiments included excess dilution using DMSO and PBSA as well as addition of polylysine, CA, or BSA. CA was used as a control with the DOTAP vesicles, since its pI is close to that of Aβ (5.9 and 5.5, respectively; *39*), while BSA and polylysine are negatively and positively charged at neutral pH, respectively.

Laurdan fluorescence spectra were obtained using the same spectrofluorometer. The fluorescence spectrum of laurdan in membranes is sensitive to phospholipid packing and phase as well as the polarity and dynamics of water molecules surrounding the dye (*40*). These spectral changes can be quantified using generalized polarization (GP) values (*40*). Four GP values were calculated using characteristic wavelengths for gel and liquid-crystalline phases per eq 2:

$$\mathrm{GP}_{\mathrm{em}(434,490)} = \frac{I_{410} - I_{340}}{I_{410} + I_{340}} \qquad (2)$$

$$\mathrm{GP}_{\mathrm{ex}(340,410)} = \frac{I_{434} - I_{490}}{I_{434} + I_{490}}$$

where I_{410} and I_{340} are the intensities of the excitation spectrum at wavelengths of 410 and 340 nm, respectively, with the emission wavelength set to 434 [$GP_{em(434)}$] or 490 nm [$GP_{em(490)}$] (*40*−*42*). Likewise, I_{434} and I_{490} are the intensities of the emission spectrum at wavelengths of 434 and 490 nm, respectively, with the excitation wavelength set to 340 [$GP_{ex(340)}$] or 410 nm [$GP_{ex(410)}$] (*40*, *43*). Laurdan GP measurements as a function of Aβ concentration or cuvette temperature were taken using the same procedures as described above.

Lifetime Fluorescence Spectroscopy. DPH fluorescence lifetimes were measured using a PTI fluorescence spectrometer equipped with a nanosecond flash lamp timed using a pulse generator from Stanford Research Systems, Inc. (Sunnyvale, CA). Data were collected for 50 scans using the strobe technique and analyzed using PTI Timemaster software. Excitation and emission wavelengths were set to 360 and 430 nm, respectively. The excitation flash profile was obtained by scattering light at 360 nm through a dilute aqueous solution of Ludox glass beads. POPC/DPH and POPG/DPH (200:1) liposomes were diluted (to ∼620 μM) using PBSA in the presence or absence of Aβ aggregated for 2 days at pH 7 (final Aβ concentration of 44.0 μM).

Differential Scanning Calorimetry. Data were collected using an MCS differential scanning calorimeter running Origin software, both from Microcal (Northampton, MA).

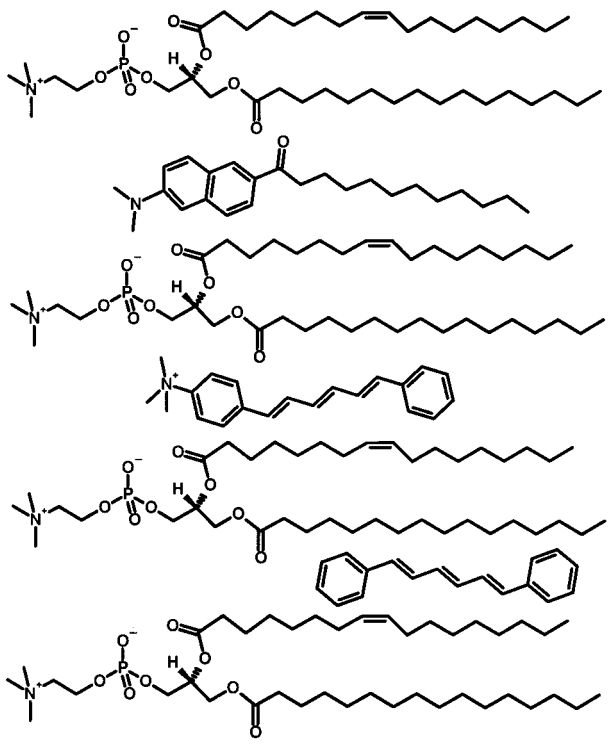

FIGURE 1: Chemical structure and approximate location in a model POPC monolayer of the fluorescent dyes laurdan, TMA-DPH, and DPH (*38*, *43*). The dimethylamino group of laurdan is reported to be located ∼5 Å from the bilayer surface (*43*). The hexatriene group of TMA-DPH and DPH are reported to be located near the C3−C4 (∼10.9 Å from the membrane center) and C9−C10 (∼7.8 Å) groups, respectively, in various PC vesicles (*38*, *47*). This figure is for illustrative purposes only and does not reflect exact dye locations.

DMPC and DMPG lipids were resuspended in PBSA at 5 mg/mL, allowed to fully hydrate (∼35−45 °C) for at least 1 h, and extruded (∼35−45 °C). The vesicles were either used immediately or stored at 4 °C until they were used. The liposomes were diluted to 0.2 mg/mL either in the presence or in the absence of Aβ aggregated for 2 days at pH 6 or 7. The final DMSO concentration in all cases was less than 1% (v/v). The reference cell was filled with an identical DMSO/PBSA solution. Samples were heated from 10 to 35 °C at 20 °C/h under N_2 gas. Generally, each sample underwent six heating and cooling cycles. Only heating scans were recorded, and scans 2−5 were typically used in data analysis.

RESULTS

We explored Aβ−membrane interactions using several fluorescent dyes that partition into distinct regions of the bilayer. The approximate locations of the fluorescent dyes used in these experiments in a model POPC monolayer are shown schematically in Figure 1. In all experiments, freshly prepared monomeric Aβ or aggregated Aβ aged for 2 days was added to the phospholipid vesicles, and responses were measured within 10−20 min. A detailed characterization of the Aβ solutions was described previously and is not repeated here (*8*).

Effect of Aβ on DPH Anisotropy in Cationic Lipid Vesicles. As reported previously, aggregated Aβ significantly increased DPH anisotropy in zwitterionic (POPC) and anionic (POPG) vesicles (*8*). Here, we report that aggregated Aβ increased

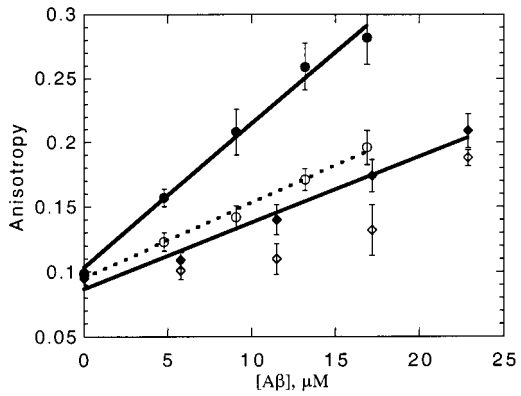

FIGURE 2: DPH anisotropy with DOTAP vesicles at pH 6 (◆ and ●) or 7 (◇ and ○) upon addition of freshly diluted Aβ (◆ and ◇) and Aβ aged for 2 days (● and ○). Aβ was dissolved in DMSO, then diluted 20-fold in PBSA (pH 6 or 7), and allowed to aggregate for 2 days at room temperature. Fluorescence intensity measurements were taken in parallel and perpendicular orientations, and anisotropy was calculated as per eq 1. The initial DOTAP vesicle concentration was 250 μM. Data are a compilation of no less than six replicate experiments. Error bars are $\pm$1 standard deviation. The slope of the regression lines are 5.8 ($\times 10^{-3}$ anisotropy unit/μM Aβ; aged for 2 days, pH 7, $r^2 = 0.94$), 11 (Aβ aged for 2 days, pH 6, $r^2 = 0.95$), and 5.1 (freshly diluted Aβ, pH 6, $r^2 = 0.93$). Freshly diluted Aβ at pH 7 showed little initial response to increasing Aβ concentration, but the response increased dramatically with time over several hours.

DPH anisotropy in cationic DOTAP vesicles in the same aggregation-dependent manner (Figure 2). Specifically, Aβ aged for 2 days in PBSA (pH 6 or 7) induced a dose-dependent increase in DPH anisotropy, with a significantly larger effect at pH 6. The concentration-dependent increase in DPH anisotropy was modeled as a linear function; the slopes of the regression lines for Aβ aged for 2 days at pH 6 and 7 were 11 and 5.8 μM^{-1}, respectively. These values are comparable to previous measurements in POPC (9 and 5.4 μM^{-1}, respectively) and POPG (10.4 and 7.7 μM^{-1}, respectively) liposomes (*8*). Monomeric Aβ added directly to DOTAP vesicles at pH 6 had a lesser, but still significant, effect on DPH anisotropy (Figure 2), which is attributed to the rapid aggregation kinetics of Aβ at acidic pH (*8, 39*). Freshly diluted Aβ at pH 7 initially caused little to no increase in DPH anisotropy of DOTAP vesicles (Figure 2), consistent with the results reported previously for POPC and POPG. However, DPH anisotropy increased slowly but steadily until the maximal value of DPH anisotropy in lipid bilayers ($\sim$0.34) was reached after several hours (data not shown). This response was unique to DOTAP with freshly diluted Aβ at pH 7; no such phenomenon was observed with POPC, POPG, type 1, or type 2 vesicles. Control solutions of BSA, CA, and polylysine had no effect on DPH anisotropy in all the phospholipids that were studied (data not shown).

Freshly diluted and aged Aβ agglomerated DOTAP into macroscopic aggregates visible to the naked eye. The time scale for agglomeration by monomeric Aβ was slow, and roughly correlated with the slow increase in DPH anisotropy. BSA (net charge of -18 at neutral pH; *44*) also agglomerated DOTAP, but with no change in DPH anisotropy, establishing that increases in anisotropy were specific to Aβ and not a byproduct of liposomal agglomeration (data not shown). CA did not increase DPH anisotropy or induce agglomeration, even though the pI of CA is very close to that of Aβ (5.9 and 5.5, respectively; *39*).

Effect of Aβ Aggregates on DPH Lifetime. Steady-state anisotropy is a function of both dye rotational correlation time (ϕ) and fluorescence lifetime (τ). This relationship is described by the Perrin equation, $r = r_o(1 + \tau/\phi)^{-1}$, where r_o represents anisotropy in a vitrified solution (*37*). We wanted to verify that observed changes in DPH steady-state anisotropy were related to changes in membrane fluidity (ϕ) rather than to environmental changes that influence the DPH fluorescence lifetime (τ). This may occur, for example, due to water penetration near the DPH dye. The mean DPH lifetime ($\langle\tau\rangle$) in POPG liposomes was 9.0 $\pm$ 0.3 ns ($n = 5$, mean $\pm$ standard deviation), consistent with literature values (*45*). In the presence of Aβ aggregated for 2 days at pH 7 [lipid:peptide ratio (L:P) = 14], the DPH lifetime was unaffected; $\langle\tau\rangle$ was 9.0 $\pm$ 0.2 ns ($n = 9$). DPH anisotropy increased approximately 0.14 units ($\sim$80% of the net change) at the same L:P ratio (*8*). Thus, in our system, the steady-state fluorescence anisotropy (r) of DPH serves as a measure of average membrane orientational order (*38*). Similar results were obtained with POPC (data not shown).

Aβ−Membrane Interactions in Liposomes That Undergo a Phase Transition. The melting temperature (T_m) of POPC, POPG, and DOTAP liposomes is low (approximately -2 to -10 °C), precluding measurements in the gel phase. To explore the effect of aggregated Aβ on gel phase lipids, we used lipids that undergo a phase transition near room temperature, namely, DMPC (T_m = 23.5 °C) and DMPG (T_m = 23.3 °C) (*46*). Aβ was aggregated for 2 days in PBSA at pH 7 (Figure 3) or pH 6 (Figure 4) and added to vesicles at the same pH value (L:$P \sim 14$, 18.5 μM Aβ). Steady-state anisotropies were measured from 10 to 40 °C. In all cases, Aβ did not discernibly shift T_m, and there was no observable hysteresis in the heating versus cooling curves. For all the systems that were studied, DPH anisotropy increased measurably in the liquid-crystalline phase and part of the transition region, but not in the gel phase. Aβ aggregated at either pH 6 or 7 induced a comparable increase in DMPC vesicles (compare Figures 3A and 4A). Aβ aggregated at pH 6 had a larger effect than Aβ at pH 7 in DMPG vesicles (compare Figures 3B and 4B, $p < 0.01$). These results were compared to the effect of temperature on DPH anisotropy in multicomponent (type 1) vesicles, which do not show a sharp phase transition. DPH anisotropy decreased linearly with temperature, from 0.29 at 12 °C to 0.20 at 40 °C. Addition of Aβ (18.5 μM) induced a consistent increase of $\sim$0.02 anisotropy units at all temperatures in this range (data not shown).

To independently verify that Aβ does not change T_m, differential scanning calorimetry (DSC) thermograms of DMPC liposomes were obtained alone or in the presence of Aβ aggregated for 2 days at pH 6 or 7 (Figure 5). Aβ aggregates did not affect the DSC trace, T_m, or ΔH of the phospholipid phase transition. ΔH values, integrated from the baseline, were 0.0017 cal with Aβ (traces A and B) and 0.0018 cal with DMPC alone (trace C). Experiments using DMPG lipids gave similar results (data not shown). In all cases, samples underwent several heating and cooling cycles with no effect on the DSC trace.

Aβ−Membrane Interactions Closer to the Membrane Surface. To further explore Aβ−membrane interactions near

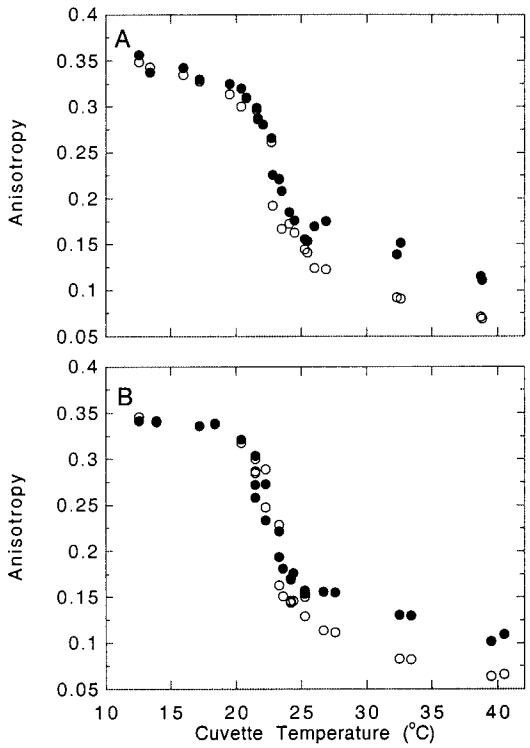

FIGURE 3: DPH anisotropy at pH 7 in (A) DMPC and (B) DMPG liposomes with aggregated Aβ (●) or PBSA control (○) as a function of cuvette temperature. Aβ was dissolved in DMSO, then diluted 20-fold in PBSA (pH 7), and allowed to aggregate for 2 days at room temperature. The final phospholipid and Aβ concentrations were 250 and 18.5 μM, respectively. Measurements were taken as described in the legend of Figure 2. Each data point is the average of two measurements. Other data sets were taken with similar results, but are not shown for clarity.

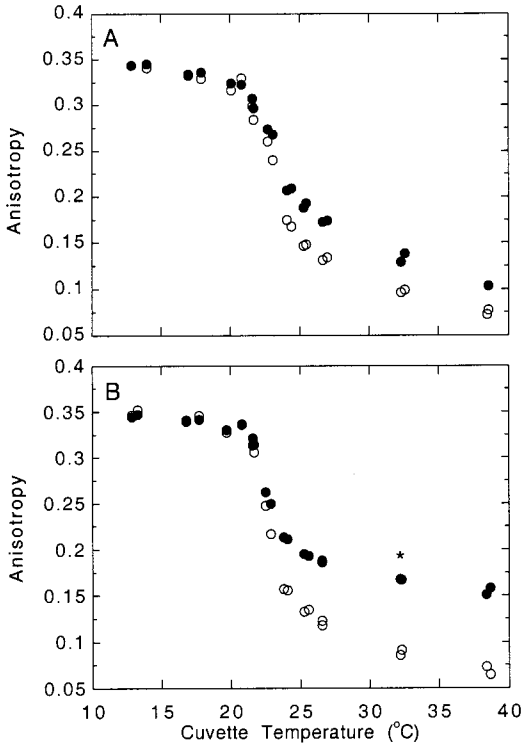

FIGURE 4: DPH anisotropy at pH 6 in (A) DMPC and (B) DMPG liposomes with aggregated Aβ (●) or PBSA control (○) as a function of cuvette temperature. Aβ was dissolved in DMSO, then diluted 20-fold in PBSA (pH 6), and allowed to aggregate for 2 days at room temperature. Each data point is the average of two measurements. Other data sets were taken with similar results, but are not shown for clarity. To evaluate statistical differences between Aβ aggregated at pH 6 or 7, data points near 33 °C were averaged into one data point and a Student's *t* test was used. Via comparison of Figures 3B and 4B, the effect on DPH anisotropy in DMPG liposomes with Aβ aged for 2 days at pH 6 is statistically larger than with Aβ aged for 2 days at pH 7 (asterisk denotes $p < 0.01$).

the glycerol backbone region, we used the hydrophilically modified dye TMA-DPH, which is located at a shallower level in the lipid bilayer due to the addition of a trimethylamino group (Figure 1; *47*). Figure 6 shows temperature scans of TMA-DPH anisotropy in DMPC and DMPG vesicles with Aβ aged for 2 days at pH 7 or PBSA controls. There was little to no effect of Aβ aggregates on TMA-DPH anisotropy, in contrast to the results with the more deeply embedded DPH (Figure 3). Aggregated Aβ also induced smaller increases in TMA-DPH anisotropy in POPC and POPG liposomes compared to DPH (data not shown).

To examine whether Aβ affected membrane properties near the bilayer surface, we employed the amphiphilic fluorescent dye laurdan, which is localized near the polar headgroups (Figure 1) and displays high sensitivity to the polarity of its environment. Changes in laurdan excitation and emission spectra due to changes in the dye's environment are quantified using the GP factor, shown in eq 2 (*40*). GP_{ex} (emission spectra taken at constant excitation wavelength) reports on the accessibility and mobility of water molecules neighboring excited-state laurdan (*48*); decreases in GP_{ex} indicate increased water accessibility and mobility. GP_{em} (excitation spectra taken at a constant emission wavelength) report on the ground-state environment of laurdan (*49*); GP_{em} decreases when laurdan−lipid interactions weaken. Photoselection of laurdan in more- or less-restricted environments is possible; for example, changes in $GP_{ex(410)}$ and $GP_{em(434)}$ without changes in $GP_{ex(340)}$ and $GP_{em(490)}$ indicate that only those laurdan molecules in a more restricted (gel-like) microenvironment are affected (*50*, *51*). GP values are wavelength-independent in the gel phase, but vary with wavelength in the liquid-crystalline state (*40*, *43*).

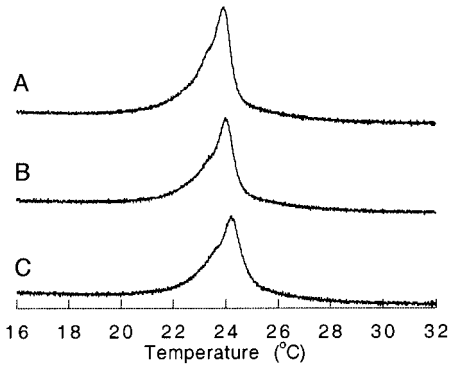

FIGURE 5: DSC heating thermograms of DMPC lipids with (A) Aβ at pH 7, (B) Aβ at pH 6, and (C) DMPC control. The reference cell was filled with an identical solution of DMSO and PBSA. DMPC liposomes and Aβ solutions were diluted to 0.2 mg/mL (295 μM) and 18.5 μM, respectively, to yield an *L*:*P* ratio of ~16:1. The fourth heating scan is shown.

$GP_{ex(340)}$ values for pure lipids were 0, −0.07, and −0.3 for POPG, POPC, and DOTAP, respectively. These results imply that the cationic DOTAP permits the greatest water penetration and/or water mobility in the headgroup region, whereas POPG allows the least. $GP_{em(434)}$ values for DOTAP

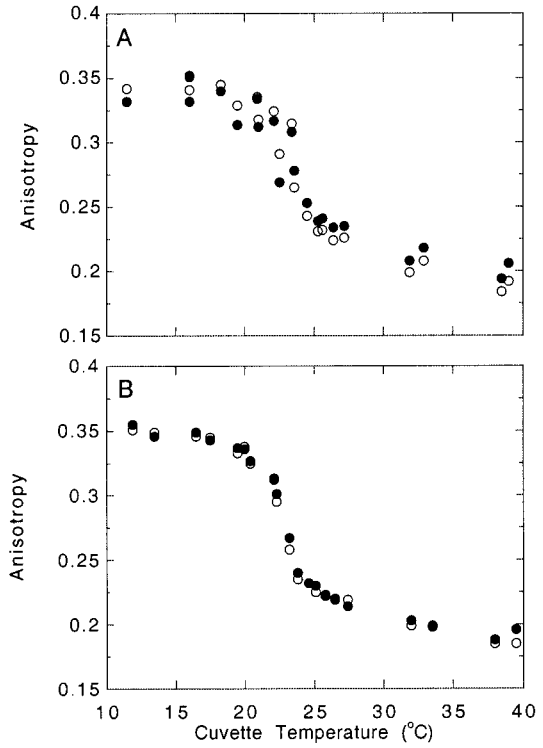

FIGURE 6: TMA-DPH anisotropy in (A) DMPC and (B) DMPG vesicles with Aβ aggregated at pH 7 (aged for 2 days) (●) or PBSA control (○) as a function of cuvette temperature. The final phospholipid and Aβ concentrations were 250 and 18.5 μM, respectively. Each data point is the average of two measurements. Other data sets were taken with similar results, but are not shown for clarity.

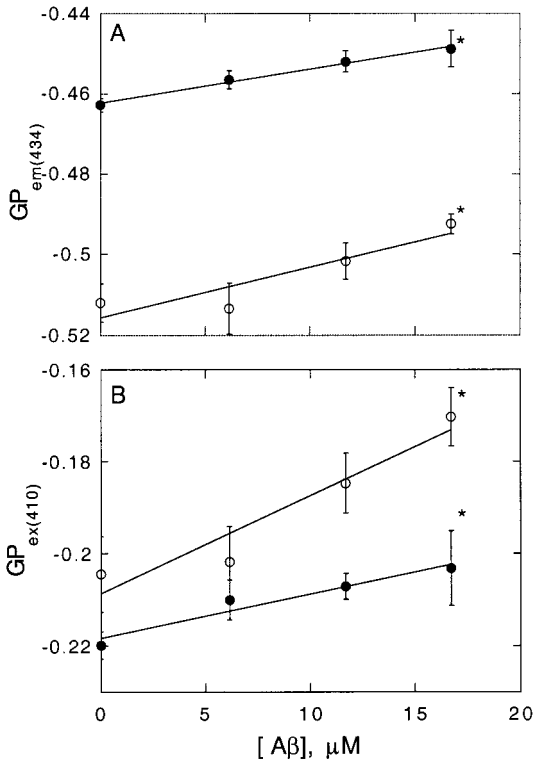

FIGURE 7: Excitation and emission generalized polarization (GP) values of the laurdan dye using an emission wavelength of 434 nm (A) or an excitation wavelength of 410 nm (B) with POPC (●) and POPG (○) liposomes. Aβ was dissolved in DMSO, then diluted 20-fold in PBSA (pH 6), and allowed to aggregate for 2 days at room temperature. GP values were calculated using eq 2. The initial phospholipid concentration was 250 μM. Error bars show the standard deviation ($n = 4$). Statistical significance between the first (0 μM Aβ) and last data points (~17 μM Aβ) was calculated using a Student's t test (asterisks denote $p < 0.05$). The effect of Aβ on $GP_{em(490)}$ and $GP_{ex(340)}$ was statistically significant with POPG but not with POPC (not shown). Other data sets were taken with similar results, but are not shown for clarity.

and POPG are similar and lower than those for POPC; this implies the zwitterionic POPC associates more strongly with laurdan than do the charged lipids (*50*). These differences are localized near the interfacial surface since the initial DPH anisotropies are very similar for all three phospholipids. In control experiments, polylysine (0.08−0.1 mg/mL) dramatically affected GP values with the anionic lipids POPG and DMPG: GP_{ex} increased by ~0.30−0.35 and GP_{em} by ~0.1−0.2. Polylysine had no observable effect on GP values of laurdan embedded in POPC or DOTAP vesicles. BSA did not affect GP values with POPC or POPG, but increased both GP_{ex} and GP_{em} with DOTAP. Buffer alone did not affect GP values in any of the lipid systems that were tested. Taken together, these results indicate that laurdan fluorescence is strongly sensitive to protein−lipid interactions near the polar headgroup region. Coulombic interactions between polylysine and the anionic PG headgroup, or BSA and the cationic DOTAP headgroup, are likely responsible for the observed increases in GP_{ex} and GP_{em}.

Since aggregated Aβ at pH 6 or 7 significantly decreased the fluidity of the bilayer interior, we asked whether the bilayer structure at the surface would be similarly affected. Freshly diluted or Aβ aggregated for 2 days at pH 7 had little to no effect on any GP value for POPC and POPG (data not shown). Aβ aggregated for 2 days at pH 6 significantly increased all four GP values for POPG; however, the magnitude of the effect was only $^1/_{10}$ of that of polylysine. With POPC, only $GP_{ex(410)}$ and $GP_{em(434)}$ increased slightly, indicating a modest effect on only those laurdan molecules in a restricted (gel-like) environment (Figure 7).

In phospholipids that undergo a phase transition near room temperature (DMPC and DMPG), Aβ aged for 2 days at pH 7 induced a very slight, but consistent, change in laurdan fluorescence only in the phase-transition region (Figure 8). The greatest changes were observed in $GP_{ex(410)}$ and $GP_{em(434)}$ (laurdan in a restricted or gel-like environment). With DOTAP, freshly diluted Aβ at pH 7 induced a time-dependent increase in GP_{ex} and GP_{em} (data not shown). The magnitude of this change was similar to that seen with polylysine and PG, or BSA and DOTAP, but the time scale was very slow and comparable to that for the increase in DPH anisotropy and agglomeration. Aβ aggregated for 2 days at pH 7 also increased GPs with DOTAP liposomes (data not shown), but the magnitude of the effect was greater with fresh Aβ than with aged Aβ. This pattern is in distinct contrast to the relative impact of fresh versus aged Aβ on anionic and zwitterionic liposomes. Aβ aged for 2 days at pH 6 or 7 did not significantly affect laurdan GP values in multicomponent type 2 liposomes (data not shown).

DISCUSSION

Steady-state DPH anisotropy has been widely used to measure lipid order (*29*, *52*) and specifically reports on phospholipid acyl chain dynamics (*38*, *53*). Increases in

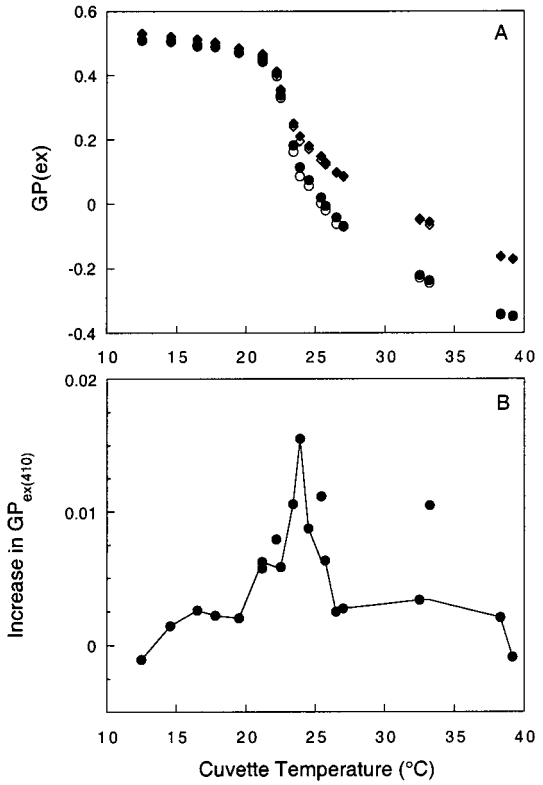

FIGURE 8: (A) Excitation GP values of laurdan in DMPG as a function of cuvette temperature. Aβ aggregated at pH 7 for 2 days (◆ and ●) or a PBSA (pH 7) control (◇ and ○) was added to phospholipid vesicles. The final Aβ and phospholipid concentrations were 18.5 and 250 μM, respectively. Excitation GPs were calculated using excitation wavelengths of 410 (● and ○) and 340 nm (◆ and ◇). GP values are wavelength-dependent in the liquid-crystalline phase but independent in the gel phase (*43*), which is seen experimentally. Each data point is the average of two measurements. Other data sets were taken with similar results, but are not shown for clarity. (B) $GP_{em(410)}$ for controls was subtracted from $GP_{em(410)}$ for Aβ samples to highlight the point that the effect of Aβ on laurdan is restricted to the pretransition and transition regime. Qualitatively similar results were obtained for emission GPs, and with DMPC (not shown).

steady-state DPH anisotropy can be attributed to (a) greater molecular order of lipids surrounding DPH and a consequent slowing in DPH rotational diffusion or (b) changes in DPH fluorescence lifetime (*37*, *45*). Since the DPH fluorescence lifetime was unaffected by aggregated Aβ, we have good evidence that the increased anisotropy is due to changes in local mobility of the lipid tail (decrease in membrane fluidity) rather than changes in the microenvironment of the dye (e.g., water penetration into the bilayer interior). Lipid peroxidation reportedly decreases the fluorescence lifetime of DPH embedded in rat cardiac mitochondrial membranes (*54*). This supports our previous conclusion that lipid peroxidation is not primarily responsible for our observed changes in membrane fluidity (*8*).

We demonstrate that equivalent changes in membrane fluidity occur upon contacting aggregated Aβ with cationic, anionic, and zwitterionic lipids. This result indicates that specific charge−charge interactions between aggregated Aβ and lipid headgroups are not required to facilitate the observed decrease in fluidity. This result contrasts with other reports indicating that Aβ interacts preferentially with acidic lipids (*55*−*57*). With the exception of ref *56*, these other studies were performed with Aβ(25−35), which has a net charge of +1 at neutral pH, and/or at low ionic strength; indeed, the electrostatic interaction was abolished by raising the ionic strength to 100 mM (*55*). All our studies were carried out at physiological ionic strength with the full-length Aβ(1−40) peptide (calculated net charge of −3 at neutral pH). We conclude that Aβ association with lipid bilayers, leading to a decrease in membrane fluidity, occurs independently of headgroup charge.

To further define the extent to which Aβ affects membrane physical properties, we employed two additional membrane-embedded fluorescent dyes: TMA-DPH and laurdan. Laurdan and DPH yield topographically distinct information about the packing and order of the lipid headgroups and tails, respectively (Figure 1; *43*). We observed little to no effect of Aβ on TMA-DPH anisotropy, consistent with results in human cortex homogenates (*9*). This is likely due to the diminished effect of Aβ at the interface as well as to the location and properties of the dye. The trimethylamino modification anchors the DPH dye, restricting its angular reorientation and increasing basal anisotropies (*47*; Figure 4 vs 7). TMA-DPH also partitions into the more fluid regions of the bilayer (*58*); TMA-DPH may migrate away from any rigid areas induced by Aβ. In contrast, DPH and laurdan partition equally between the phases (*51*, *59*).

Results with control solutions of polylysine and BSA imply that shifts in laurdan fluorescence spectra are indicators of association of protein and/or polypeptide with the membrane surface, primarily due to charge−charge interactions. Both polylysine (with anionic lipids) and BSA (with cationic lipids) interacted strongly with lipid headgroups, as detected by large changes in laurdan GPs, without affecting the motion of acyl chains in the interior, as indicated by the lack of change in DPH anisotropy. Aggregated Aβ behaved in a qualitatively different manner. In several cases, no effect on laurdan GPs was observed. In those cases where an increase in laurdan GP values was observed, the magnitude of the increase was only a small fraction of that observed with polylysine or BSA. In all these cases, however, aggregated Aβ caused a significant increase in DPH anisotropy. These data imply that aggregated Aβ interacts with membranes in a manner quite distinct from that of polylysine or BSA, and that substantial stable binding of Aβ to the surface is not required for loss of acyl chain mobility in the interior. We speculate that Aβ preferentially becomes buried in the membrane interior and restricts angular motion of the acyl chains (possibly due to crowding effects and/or to Aβ−acyl chain association), but has little to no substantial localization at the membrane surface.

The inability of Aβ to affect membrane fluidity in the gel phase suggests that Aβ cannot intercalate into more rigid, well-ordered bilayers. Similar behavior has been observed in other peptide/lipid systems (*60*). It is interesting to contrast Aβ with cholesterol: both increase DPH anisotropy in the liquid-crystalline phase, but only cholesterol decreases anisotropy in the gel phase (*61*). The laurdan results in DMPC and DMPG vesicles provide further hints that Aβ aggregates cannot intercalate into gel phase lipid bilayers. The greatest effects were observed near T_m, where Aβ slightly but consistently increased the GP values, especially GPs associated with a gel-like microenvironment. However, the effect of Aβ at the hydrophobic core, as evidenced by DPH

anisotropy, was still muted until the temperature was sufficiently higher than the T_m. We speculate that this reflects a progressive insertion of Aβ aggregates into the hydrophobic center as the membrane becomes more fluid.

We utilized DSC to independently verify that Aβ does not change the lipid phase-transition T_m or ΔH (Figure 5). The effect of proteins on the thermotropic phase behavior of a lipid bilayer is a function of the association mechanism. For example, polylysine strongly associates with the surface of anionic lipids and increases T_m and ΔH (*62*). In contrast, insertion proteins typically have no effect on T_m and decrease ΔH only at high protein:lipid ratios (*62*). Protein and/or peptide penetration into membranes can occur independently of lipid headgroup charge (*63*), and integral membrane proteins induce marked effects on local membrane organization with only minor effects on phase behavior (*64*). Thus, the pattern observed with Aβ is characteristic of other peptide and/or protein/membrane systems in which the dominant attractive force is hydrophobic and the predominant peptide contact is with the hydrophobic core of the membrane.

At pH 7, Aβ has a negative net charge, and freshly diluted Aβ interacts only with the cationic DOTAP. Both Aβ and BSA induce agglomeration of DOTAP liposomes. These phenomena are likely a direct result of Coulombic attraction. It is interesting to note, however, that agglomeration of DOTAP with Aβ is much slower than with BSA, and that freshly diluted Aβ but not BSA increased DPH anisotropy in DOTAP. Changes in laurdan spectra and in DPH anisotropy caused by Aβ were similarly slow. We speculate that these data imply charge-mediated binding of monomeric Aβ to the DOTAP headgroups, followed by slow aggregation and/or penetration into the interior, the latter driven by hydrophobic partitioning.

On the basis of results reported here and previously (*8*), we envision the following scenario. Spontaneous self-association of Aβ in solution produces fibrillar aggregates in which the accessible surface charge is reduced, but the number of large solvent-exposed hydrophobic patches is increased. (Coalescence of some hydrophobic side chains into solvent-exposed patches could occur during Aβ self-association even with an overall reduction in the total number of solvent-exposed hydrophobic side chains.) This hypothesis is supported by the following results. (a) On the basis of data from the laurdan assay, monomeric Aβ (net charge of -3) interacted strongly with cationic lipids, but not at all with neutral or anionic lipids, while aggregated Aβ produced little effect regardless of headgroup charge. (b) The fluorescence intensity of bis-ANS, a dye that binds to large, solvent-exposed hydrophobic patches, increased as Aβ aggregation proceeded (*8*). (c) Garzon-Rodriguez and coworkers reported a progressive increase in the level of water exposure of the 40th residue of Aβ, which lies in the hydrophobic membrane insertion region of APP, upon aggregation (*65*). We propose that Aβ aggregates bind weakly or not at all to polar headgroups on lipid bilayer surfaces. However, there is a thermodynamic driving force for partitioning into the bilayer interior to bury solvent-exposed hydrophobic patches on the aggregate surface. Such burial leads to localized crowding which increases the driving force for ordering of lipid tails. In the gel phase, partitioning is limited by the rigidity of the lipid bilayer, restricting access to the interior.

The relevance of the observed effects of Aβ on membrane structure to AD pathology is unknown. Eckert et al. (*66*) report that fluidity of hippocampal membranes in AD brains is reduced, and decreases in mitochondrial membrane fluidity were greater in AD patients than in age-matched controls (*67*). Regulation of membrane fluidity is important for proper functioning of integral membrane proteins and signal transduction pathways. For example, decreased membrane fluidity disrupts the CCK receptor−G protein complex in rat cortical membranes (*68*) and alters Na^+/K^+-ATPase activity in dog brain synaptosomal plasma membranes (*69*). To ascertain whether the observed physical changes in membrane structure have important biological outcomes relevant to AD, it will be necessary to show impairment of neuronal functioning as a consequence of Aβ-mediated decreases in cell membrane fluidity.

ACKNOWLEDGMENT

We are grateful to Jeremy Bartlett and Professor Gilherme Indig for use of their lifetime fluorescence spectrometer and technical assistance. Calorimetry data were obtained at the University of Wisconsin−Madison Biophysics Instrumentation Facility with help from Dr. Darrell McCaslin.

REFERENCES

1. Pike, C. J., Burdick, D., Walencewicz, A. J., Glabe, C. G., and Cotman, C. W. (1993) *J. Neurosci. 13*, 1676−1687.
2. Simmons, L. K., May, P. C., Tomaselli, K. J., Rydel, R. E., Fuson, K. S., Brigham, E. F., Wright, S., Lieberburg, I., Becker, G. W., Brems, D. N., and Li, W. (1994) *Mol. Pharmacol. 45*, 373−379.
3. Mattson, M. P. (1997) *Physiol. Rev. 77*, 1081−1132.
4. Iverson, L. L., Mortishire-Smith, R. J., Pollack, S. J., and Shearman, M. S. (1995) *Biochem. J. 311*, 1−16.
5. Kanfer, J. N., Sorrentino, G., and Sitar, D. S. (1999) *Neurochem. Res. 24*, 1621−1630.
6. Torp, R., Head, E., Milgram, N. W., Hahn, F., Ottersen, O. P., and Cotman, C. W. (2000) *Neuroscience 96*, 495−506.
7. Yamaguchi, H., Maat-Schieman, M. L., van Duinen, S. G., Prins, F. A., Neeskens, P., Natte, R., and Roos, R. A. (2000) *J. Neuropathol. Exp. Neurol. 59*, 723−732.
8. Kremer, J. J., Pallitto, M. P., Sklansky, D. J., and Murphy, R. M. (2000) *Biochemistry 39*, 10309−10318.
9. Müller, W. E., Eckert, G. P., Scheuer, K., Cairns, N. J., Maras, A., and Gattaz, W. F. (1998) *Amyloid 5*, 10−15.
10. Avdulov, N. A., Chochina, S. V., Igbavboa, U., O'Hare, E. O., Schroeder, F., Cleary, J. P., and Wood, W. G. (1997) *J. Neurochem. 68*, 2086−2091.
11. Mason, R. P., Jacob, R. F., Walter, M. F., Mason, P. E., Avdulov, N. A., Chochina, S. V., Igbavboa, U., and Wood, W. G. (1999) *J. Biol. Chem. 274*, 18801−18807.
12. Butterfield, D. A., Yatin, S. M., Varadarajan, S., and Koppal, T. (1999) *Methods Enzymol. 309*, 746−768.
13. Lin, H., Zhu, Y. J., and Lal, R. (1999) *Biochemistry 38*, 11189−11196.
14. Hirakura, Y., Lin, M. C., and Kagan, B. L. (1999) *J. Neurosci. Res. 57*, 458−466.
15. Koudinov, A. R., Berezov, T. T., and Koudinova, N. V. (1998) *FASEB J. 12*, 1097−1099.
16. Singh, I. N., Sorrentino, G., and Kanfer, J. N. (1998) *Neurochem. Res. 23*, 1225−1232.
17. Lehtonen, J. Y., Holopainen, J. M., and Kinnunen, P. K. (1996) *Biochemistry 35*, 9407−9414.
18. McLaurin, J., Franklin, T., Fraser, P. E., and Chakrabarrty, A. (1998) *J. Biol. Chem. 273*, 4506−4515.
19. Terzi, E., Hölzemann, G., and Seelig, J. (1997) *Biochemistry 36*, 14845−14852.

20. Choo-Smith, L. P., Garzon-Rodriguez, W., Glabe, C. G., and Surewicz, W. K. (1997) *J. Biol. Chem. 272*, 22987−22990.
21. Lane, N. J., Balbo, A., Fukuyama, R., Rapoport, S. I., and Galdzicki, Z. (1998) *J. Neurocytol. 27*, 707−718.
22. Yang, A. J., Chandswangbhuvana, D., Margol, L., and Glabe, C. G. (1998) *J. Neurosci. Res. 52*, 691−698.
23. Pillot, T., Goethals, M., Vanloo, B., Talussot, C., Brasseur, R., Vandekerckhove, J., Rosseneu, M., and Lins, L. (1996) *J. Biol. Chem. 271*, 28757−28765.
24. Vargas, J., Alarcon, J. M., and Rojas, E. (2000) *Biophys. J. 79*, 934−944.
25. Matsuzaki, K., and Horikiri, C. (1999) *Biochemistry 38*, 4137−4142.
26. McLaurin, J., and Chakrabartty, A. (1996) *J. Biol. Chem. 271*, 26482−26489.
27. Good, T., and Murphy, R. M. (1995) *Biochem. Biophys. Res. Commun. 207*, 209−215.
28. Hirakura, Y., Satoh, Y., Hirashima, N., Suzuki, T., Kagan, B. L., and Kirino, Y. (1998) *Biochem. Mol. Biol. Int. 46*, 787−794.
29. Van Ginkel, G., Van Langen, H., and Levine, Y. K. (1989) *Biochimie 71*, 23−32.
30. Lentz, B. R., Barenholz, Y., and Thompson, T. E. (1976) *Biochemistry 15*, 4521−4528.
31. Prendergast, F. G., Haugland, R. P., and Callahan, P. J. (1981) *Biochemistry 20*, 7333−7338.
32. Weber, G., and Farris, F. J. (1979) *Biochemistry 18*, 3075−3078.
33. Chong, P. L. (1988) *Biochemistry 27*, 399−404.
34. Mills, J., and Reiner, P. B. (1999) *J. Neurochem. 72*, 443−460.
35. Shen, C. L., and Murphy, R. M. (1995) *Biophys. J. 69*, 640−651.
36. Snyder, S. W., Ladror, U. S., Wade, W. S., Wang, G. T., Barrett, L. W., Matayoshi, E. D., Huffaker, H. J., Krafft, G. A., and Holzman, T. F. (1994) *Biophys. J. 67*, 1216−1228.
37. Lakowicz, J. R. (1986) *Principles of Fluorescence Spectroscopy*, Plenum Press, New York.
38. Lentz, B. R. (1989) *Chem. Phys. Lipids 50*, 171−190.
39. Wood, S. J., Maleeff, B., Hart, T., and Wetzel, R. (1996) *J. Mol. Biol. 256*, 870−877.
40. Parasassi, T., De Stasio, G., d'Ubaldo, A., and Gratton, E. (1990) *Biophys. J. 57*, 1179−1186.
41. Parasassi, T., De Stasio, G., Ravagnan, G., Rusch, R. M., and Gratton, E. (1991) *Biophys. J. 60*, 179−189.
42. Hirsch-Lerner, D., and Barenholz, Y. (1999) *Biochim. Biophys. Acta 1461*, 47−57.
43. Antollini, S. S., and Barrantes, F. J. (1998) *Biochemistry 37*, 16653−16662.
44. Peters, T., Jr. (1985) *Adv. Protein Chem. 37*, 161−245.
45. Muller, J. M., van Ginkel, G., and van Faassen, E. E. (1996) *Biochemistry 35*, 488−497.
46. Encinar, J. A., Fernandez, A. M., Gavilanes, F., Albar, J. P., Ferragut, J. A., and Gonzalez-Ros, J. M. (1996) *Biophys. J. 71*, 1313−1323.
47. Kaiser, R. D., and London, E. (1998) *Biochemistry 37*, 8180−8190.
48. Viard, M., Gallay, J., Vincent, M., Meyer, O., Robert, B., and Paternostre, M. (1997) *Biophys. J. 73*, 2221−2234.
49. Bagatolli, L. A., Parasassi, T., Fidelio, G. D., and Gratton, E. (1999) *Photochem. Photobiol. 70*, 557−564.
50. Bagatolli, L. A., Gratton, E., and Fidelio, G. D. (1998) *Biophys. J. 75*, 331−341.
51. Parasassi, T., Ravagnan, G., Rusch, R. M., and Gratton, E. (1993) *Photochem. Photobiol. 57*, 403−410.
52. Schroeder, F. (1988) *Methods for Studying Membrane Fluidity. Advances in Membrane Fluidity*, Vol. 1, pp 193−219, Alan R. Liss Inc., New York.
53. Lentz, B. R. (1993) *Chem. Phys. Lipids 64*, 99−116.
54. Koyama, T., Zhu, M. Y., Shong, L. Q., Nakabayashi, T., Keatisuwan, W., Kinjo, M., and Araiso, T. (1990) *Jpn. J. Physiol. 40*, 635−649.
55. Terzi, E., Holzemann, G., and Seelig, J. (1994) *Biochemistry 33*, 7434−7441.
56. McLaurin, J., and Chakrabartty, A. (1997) *Eur. J. Biochem. 245*, 355−363.
57. Chauhan, A., Ray, I., and Chauhan, V. P. S. (2000) *Neurochem. Res. 25*, 423−429.
58. Parente, R. A., and Lentz, B. R. (1985) *Biochemistry 24*, 6178−6185.
59. Lentz, B. R., Barenholz, Y., and Thompson, T. E. (1976) *Biochemistry 15*, 4529−4537.
60. Zwaal, R. F., Comfurius, P., and Bevers, E. M. (1998) *Biochim. Biophys. Acta 1376*, 433−453.
61. Borenstain, V., and Barenholz, Y. (1993) *Chem. Phys. Lipids. 64*, 117−127.
62. McElhaney, R. N. (1986) *Biochim. Biophys. Acta 864*, 361−421.
63. Davletov, B., Perisic, O., and Williams, R. L. (1998) *J. Biol. Chem. 273*, 19093−19096.
64. Gil, T., Ipsen, J. H., Mouritsen, O. G., Sabra, M. C., Sperotto, M. M., and Zuckerman, M. J. (1998) *Biochim. Biophys. Acta 1376*, 245−266.
65. Garzon-Rodriguez, W., Vega, A., Sepulveda-Becerra, M., Milton, S., Johnson, D. A., Yatsimirsky, A. K., and Glabe, C. G. (2000) *J. Biol. Chem. 275*, 22645−22649.
66. Eckert, G. P., Cairns, N. J., Maras, A., Gattaz, W. F., and Müller, W. E. (2000) *Dementia Geriatr. Cognit. Disord. 11*, 181−186.
67. Mecocci, P., Beal, M. F., Cecchetti, R., Polidori, M. C., Cherubini, A., Chionne, F., Avellini, L., Romano, G., and Senin, U. (1997) *Mol. Chem. Neuropathol. 31*, 53−64.
68. Rinken, A., Harro, J., Engström, L., and Oreland, L. (1998) *Biochem. Pharmacol. 55*, 423−431.
69. Deliconstantinos, G. (1985) *Neurochem. Res. 10*, 1605−1613.

BI010417X